Tuning of a tracking multi-parametric predictive controller using local linear analysis

Samo Gerkšič, Boštjan Pregelj

Dept. of Systems and Control, Jozef Stefan Institute, Jamova 39, Ljubljana, Slovenia

E-mail: samo.gerksic@ijs.si, bostjan.pregelj@ijs.si

ABSTRACT

Multi-parametric model predictive control (mp-MPC) makes possible the application of MPC controllers with a low on-line computational demand and rapid sampling. It is appealing for low-level control applications, where the disturbance-rejection properties are very important. This study explores two important issues in the transition from mp-MPC theory to the implementation of an industrial controller: offset-free output-feedback tracking, and controller tuning based on local linear analysis of the closed-loop system. An experimental case study on a two-input single-output system for pressure control in the vacuum chamber of a wire annealer is presented.

Keywords: Predictive control; Kalman filters; Tracking; Tuning characteristics; Linear analysis; Control applications; Pressure control

1 Introduction

Industrial MPC is mostly associated with control of large-scale multivariate processes that have relatively slow dynamics, where it is used in the mid-layer of the control hierarchy [1]. Its advantages, such as the advanced constraints handling and the straightforward implementation of feedforward control, are also welcome for low-level control; however, such applications are relatively rare. This is mainly due to the computing requirements of on-line optimization. In a growing number of demanding control loops, PID controllers have been replaced by simplified predictive controllers, most notably Predictive Functional Control (PFC) [2]. However, such methods typically lack the full constraints handling and have weak analysis support.

The recently developed multi-parametric (explicit) MPC approach [3], [4], [5], [6] avoids the need for on-line optimization by computing the complete solution to the MPC control problem parametrically in advance, at the stage of controller design. A state partition table is generated, comprising polyhedral critical regions, with each region being characterized by a set of active constraints and a local affine state control law. This allows the MPC control law to be interpreted as a hybrid or variable-structure controller, which is equivalent to the underlying on-line MPC controller. The remaining on-line computation with mp-MPC includes a region-search algorithm and a state-vector multiplication with the selected row of the partition table. The computation may be implemented on industrial standard programmable-logic controllers, inexpensive microcontrollers, or FPGA chips [7]. The mp-MPC approach is limited to small-scale MPC problems due to the parametric explosion of the off-line computation demand, most notably with the number of control-signal parameters and the number of possible combinations of active constraints [8].

The majority of the mp-MPC literature addresses theoretical issues that assume the state-feedback control, which are often of limited practical applicability. The publicly available mp-MPC software libraries Multi-parametric Toolbox (MPT) [9], [10] and Hybrid Toolbox (HT) [11] enable offset-free tracking of reference signals by applying *velocity-tracking augmentation* of the model. In mp-MPC, the time-varying reference signals appear as additional parameters of the multi-parametric controller, undesirably increasing the size of the off-line optimization problem; with fixed target values this may be avoided by applying simple coordinate shifts. However, this form of tracking does not remove offset with *integrating* disturbances (asymptotically non-zero disturbances [12], such as: offset, drift, etc.).

Several approaches to the removal of steady-state offset with integrating disturbances may be found in the application-oriented mp-MPC literature that considers output feedback, for example [13], [11], [14], and the POP toolbox of ParOS Parametric Solutions Ltd., however the implementations tend to depart from the mainstream MPC approaches. One possible approach is *Tracking Error Integration* (TEI). With TEI, the process model is first augmented with the reference signal state y_r so that the new output becomes the tracking error ($y_r - y$); then, an integrator state e_{TEI} that integrates the tracking error is appended [11], [13]. The TEI scheme is prone to integrator windup when the set-points are unreachable; protection is required. Further, the modification to the cost function for significant integral action may adversely affect the nominal tracking performance in the form of overshoots, similarly as with PI control [15]. *Disturbance Estimation* (DE) is an alternative approach which is more commonly used in traditional MPC. With DE, an integrating disturbance state(s) is appended to the model (*disturbance augmentation*), and an observer or estimator is used to estimate the appended state(s) or the whole augmented state. In the simplest form of DE with the traditional output-step-disturbance (OSD) model, an open-loop observer is used for the basic model and a dead-beat estimator is used for the disturbance state(s) appended at the outputs. In more general DE formulations [16], [17], [18], [12], state estimation of the disturbance-augmented state is used. Multi-parametric moving-horizon estimators, which are dual to mp-MPC controllers, are also under development, but their off-line computational complexity is high [19], [20]. In some DE variants, for example [21], [22], the integrator of the tracking velocity form is also used in disturbance estimation; however, rate constraints must then be handled separately from the disturbance-affected integrator states.

DE may be implemented in a *"joint" scheme* or a *Target Calculator (TC) scheme*. In the "joint" scheme, the MPC controller integrates the functions of constrained dynamic control and offset-free tracking, which is implemented by the velocity-tracking model augmentation and the tracking form of the cost function over a finite horizon. In the alternative TC scheme ([23], [24], [5]; [12], [25]), the MPC controller is decomposed into the asymptotic steady-state target calcualtor (TC) component (in charge of offset-free tracking) and the MPC "dynamic controller" (DC) (in charge of transient dynamics about the operating point). In the following sections, the joint scheme is chosen and described in detail; however no decisive practical performance difference was found in our case study and this choice is due to methodological preferences [15]. Due to the artificial decomposition of the MPC problem, the TC is blind to transient infeasibilities, which arise later in the DC, for example due to rate constraints [26]. In practice, reference pre-processing, back-off from the constraints, or a fall-back feasibility recovery controller may be used to overcome this problem. However, this complicates the structure of the control law and the analysis of constrained performance. An enhanced TC scheme exists where the target and the DC decision variables are being determined at once so that the artificial decomposition is removed [27]; unfortunately this increases the computational load, while our preference was a simple scheme that facilitates full handling of constraints over longer predictive horizons.

In this paper we discuss the implementation of a "joint"-scheme DE-based mp-MPC controller suitable for engineering applications such as PID controller replacement. It is shown that output feedback may be handled with standard DE approaches known from conventional MPC, for example [1], [16], [17], [12], [5], [28], [21]. Local linear analysis (LLA) of a closed-loop system with such a controller is presented. We show how efficient control of a non-square plant with redundant control inputs may be implemented with the joint-scheme mp-MPC controller (without a TC). The approach is illustrated with an experimental case-study where the mp-MPC controller is applied for pressure control of a plasma annealer, a two-input single-output system. The role of LLA in tuning for efficient feedback performance and robustness to modelling error is described.

2 Mp-MPC control using joint scheme

The joint scheme is made using an integrated mp-MPC controller, based on the constrained finite-time optimal control problem, with extensions for reference tracking and disturbance estimation. The extensions in this form are not available in the mp-MPC toolboxes MPT, HT, and POP.

The nominal discrete-time state-space plant model is

$$x(k+1) = Ax(k) + Bu(k) + Gw(k), \quad y(k) = Cx(k) + v(k) \qquad (1)$$

where $x \in \Re^{n_x}$, $u \in \Re^{n_u}$, $y \in \Re^{n_y}$; $w \in \Re^{n_w}$ and $v \in \Re^{n_y}$ are white-noise signals, and G may be used to specify the access of the noise to the state (by default, $G = I_{n_x}$); k is the sample index. Normally, this scheme is suitable for square plants ($n_u = n_y$). This model is augmented with a DE integrator state $d \in \Re^{n_d}$ with the associated white-noise signal $w_d \in \Re^{n_d}$, so that the augmented state is $x_a(k) = [x^T(k)\ d^T(k)]^T$ with the noise signal $w_a(k) = [w^T(k)\ w_d^T(k)]^T$. In the case of disturbance augmentation at the output, the disturbance-augmented system is

$$\begin{bmatrix} x(k+1) \\ d(k+1) \end{bmatrix} = \begin{bmatrix} A & 0 \\ 0 & I \end{bmatrix} \begin{bmatrix} x(k) \\ d(k) \end{bmatrix} + \begin{bmatrix} B \\ 0 \end{bmatrix} u(k) + \begin{bmatrix} G & 0 \\ 0 & I \end{bmatrix} \begin{bmatrix} w(k) \\ w_d(k) \end{bmatrix} \quad (2)$$
$$y(k) = \begin{bmatrix} C & I \end{bmatrix} \begin{bmatrix} x(k) \\ d(k) \end{bmatrix} + v(k)$$

while in the case of disturbance augmentation at the input it is

$$\begin{bmatrix} x(k+1) \\ d(k+1) \end{bmatrix} = \begin{bmatrix} A & B \\ 0 & I \end{bmatrix} \begin{bmatrix} x(k) \\ d(k) \end{bmatrix} + \begin{bmatrix} B \\ 0 \end{bmatrix} u(k) + \begin{bmatrix} G & 0 \\ 0 & I \end{bmatrix} \begin{bmatrix} w(k) \\ w_d(k) \end{bmatrix} \quad (3)$$
$$y(k) = \begin{bmatrix} C & 0 \end{bmatrix} \begin{bmatrix} x(k) \\ d(k) \end{bmatrix} + v(k)$$

with the noise covariance matrices Q_K = E$\{w_a w_a^T\}$ and R_K = E$\{vv^T\}$, respectively, assuming E$\{w_a v^T\}$ = 0. Detectability limitations must be considered [17], [12]. In both cases a compact description of the disturbance-augmented model is

$$\begin{aligned} x_a(k+1) &= A_a x_a(k) + B_a u(k) + G_a w_a(k) \\ y(k) &= C_a x_a(k) + v(k) \end{aligned} \quad (4)$$

The steady-state Kalman filter (KF) is used for state estimation with the disturbance-augmented model

$$\begin{aligned} x_a(k|k-1) &= A_a x_a(k-1|k-1) + B_a u(k-1) \\ x_a(k|k) &= x_a(k|k-1) + M_K \left[y(k) - C_a x_a(k|k-1) \right] \end{aligned} \quad (5)$$

where M_K is determined by the steady-state solution of a Riccati equation from the noise covariance matrices Q_K and R_K.

For reference tracking, the joint scheme requires the velocity form (regardless of the presence of rate constraints) and the y_r tracking parameter. This may be achieved either by velocity-and-tracking augmentation of the model (as in the MPT toolbox, for example) or by an extension of the cost-function formulation (POP toolbox). This implementation uses an approach similar to the one used by the MPT, but with the modification that velocity-and-tracking augmentation made on the disturbance-augmented model. The disturbance-velocity augmented model $\{A_{av}, B_{av}, C_{av}, G_{av}\}$, with the state $x_{av} = \left[x^T \ \ d^T \ \ u^T(k-1) \right]^T$, is made by appending the disturbance-augmented model with a noise-free integrator at the input. The disturbance-velocity-tracking augmented model, with the state $x_{avt} = \left[x^T \ \ d^T \ \ u^T(k-1) \ \ y_r^T \right]^T$, adds the reference signal y_r as an additional uncontrollable state, so that a tracking controller may be formulated using suitably constructed cost matrices as in the function mpt_yalmipTracking of the MPT toolbox [9].

In the following, we outline the formulation of the MPC controller, similar to [21] but with a different model augmentation approach. A multi-step prediction $y_N(k)$ for the prediction horizon k+1, ..., k+N and the control horizon k, ..., k+N_u–1 is

$$
\begin{aligned}
y_N(.\,|\,k) &= \left[y^T(k+1\,|\,k),\ldots,y^T(k+N\,|\,k)\right]^T \\
&= N_N x_{av}(k\,|\,k) + S_N \Delta u_{N_u}(k)
\end{aligned}
\tag{6}
$$

where $\Delta u_{N_u}(k) = \left[\Delta u^T(k),\cdots,\Delta u^T(k+N_u-1)\right]^T$, and suitable matrices N_N and S_N are constructed by stacking the consecutive prediction equations for $y(k+1\,|\,k)$, ..., $y(k+N\,|\,k)$ [21]. The future reference is assumed to be constant over the horizon and not known in advance

$$
y_{r,N}(.\,|\,k) = [\underbrace{I_{n_y},\ldots,I_{n_y}}_{N}]^T y_r(k) = I_{r_N} y_r(k)
\tag{7}
$$

The MPC cost function is defined as

$$
J\left(k,\Delta u_{N_u}(k)\right) = e_N^T(.\,|\,k)\underline{Q}_y e_N(.\,|\,k) + \Delta u_{N_u}^T(k)\underline{R}_{\Delta u}\Delta u_{N_u}(k)
\tag{8}
$$

where $\underline{Q}_y = \mathrm{diag}(\underbrace{Q_y,\ldots,Q_y}_{N})$ and $\underline{R}_{\Delta u} = \mathrm{diag}(\underbrace{R_{\Delta u},\ldots,R_{\Delta u}}_{N_u})$ are the expanded cost matrices, and the prediction of the tracking error $e = y - y_r$ over the whole predictive horizon $e_N(.\,|\,k)$ is

$$
e_N(.\,|\,k) = N_N x_{av}(k\,|\,k) + S_N \Delta u_{N_u}(k) - I_{r_N} y_r(k)
\tag{9}
$$

The unconstrained solution of the MPC control law may be obtained easily without having to compute the full multi-parametric solution, and is valuable in the early stages of controller tuning. In the absence of constraints, the control-law optimizer $\Delta u_{N_u}^*(k)$ is found analytically by inserting (9) into (8) and deriving with respect to $\Delta u_{N_u}(k)$. It has the form of a least-squares problem

$$
\Delta u_{N_u}^*(k) = \left(S_N^T \underline{Q}_y S_N + \underline{R}_{\Delta u}\right)^{-1} S_N^T \underline{Q}_y \left(y_{r,N}(.|k) - N_N x_{av}(k|k)\right)
\tag{10}
$$

If the disturbance-velocity-tracking augmented state vector x_{avt} is used, it is computed as

$$
\Delta u_{N_u}^*(k) = \left(S_N^T \underline{Q}_y S_N + \underline{R}_{\Delta u}\right)^{-1} S_N^T \underline{Q}_y \begin{bmatrix} -N_N & I_{r_N} \end{bmatrix} x_{avt}(k|k)
\tag{11}
$$

With receding-horizon control, the control becomes

$$
\begin{aligned}
\Delta u(k) &= K_C y_{r,N}(.\,|\,k) - K_C N_N x_{av}(k\,|\,k) \\
&= K_C \begin{bmatrix} -N_N & I_{r_N} \end{bmatrix} x_{avt}(k\,|\,k)
\end{aligned}
\tag{12}
$$

where the controller gain K_C is defined as

$$
K_C = \begin{bmatrix} I_{n_u} & 0 & \cdots & 0 \end{bmatrix} \left(S_N^T \underline{Q}_y S_N + \underline{R}_{\Delta u}\right)^{-1} S_N^T \underline{Q}_y
\tag{13}
$$

The full mp-MPC solution requires the minimisation of the cost (8) subject to the specified constraints on the process signals within the predictive horizon, with respect to $\Delta u_{N_u}(k)$ and as a piecewise-affine function of the augmented state vector x_{avt} [4], where the feasible parameter space of x_{avt} is divided into a finite number of polyhedral critical regions CR^i. This problem is reformulated as a multi-parametric quadratic program (mp-QP) and solved using an mp-QP solver ([9]; [11]; [29]). The optimizer obtained by mp-QP is then rearranged into the following form

$$\Delta u^{*}_{N_u}(k) = F^{i}_{x} x_{av}(k\,|\,k) + F^{i}_{r} y_r(k) + G^{i} \quad \text{when } x_{avt} \in CR^{i} \quad (14)$$

where $F^{i}_{x} \in \Re^{N_u n_u \times (n_x+n_d+n_u)}$, $F^{i}_{r} \in \Re^{N_u n_u \times n_y}$, $\left[F^{i}_{x}\ F^{i}_{r}\right] = F^{i}$, $G^{i} \in \Re^{N_u n_u \times 1}$, and the receding-horizon control law is

$$\Delta u(k) = f^{i}_{x} x_{av}(k\,|\,k) + f^{i}_{r} y_r(k) + g^{i} \quad \text{when } x_{avt} \in CR^{i} \quad (15)$$

where $f^{i}_{x} \in \Re^{n_u \times (n_x+n_d+n_u)}$, $f^{i}_{r} \in \Re^{n_u \times n_y}$, $\left[f^{i}_{x}\ f^{i}_{r}\right] = f^{i}$, and $g^{i} \in \Re^{n_u \times 1}$. The control scheme comprising the process represented by the *true model* $\{A_a^*, B_a^*, C_a^*, G_a^*\}$, the mp-MPC controller, the estimator, and the velocity augmentation is shown in Fig. 1.

*** FIG 1 HERE ***

2.1 Local linear analysis (LLA)

LLA is based on closed-loop system dynamics from the inputs $w_a(k)$, $v(k)$, and $y_r(k)$ to the noise-free output $y_{\mathrm{nf}}(k)$ [30]. Whereas the controller and the estimator are designed using the nominal model, analysis is also possible with a different true model ([31], p. 402). Further, analysis may be performed with a set of candidate true models.

Closed-loop system dynamics are obtained by blending thecontrol law (15), the estimator (5), and the true model $\{A_a^*, B_a^*, C_a^*, G_a^*\}$ (4). Velocity augmentation is applied to both the true model and the estimator model, so that the controller output $\Delta u(k)$ matches the inputs of the true model $\{A_{av}^*, B_{av}^*, C_{av}^*, G_{av}^*\}$ and the estimator $\{A_{av}^*, B_{av}^*, C_{av}^*, G_{av}^*; M_{Kv}\}$, and the estimator output $x_{av}(k\,|\,k) = \left[x_a^T(k\,|\,k) \quad u^T(k-1)\right]^T$ matches the controller input. The implementation of the augmentation is similar to eq. (3), except that there is no access of noise to the added integrator state $u(k–1)$, so $M_{Kv} = \left[M_K^T \quad 0^T_{n_u \times n_y}\right]^T$. The closed-loop system in the state-space form is made by combining the state update equations for the true model state $x_{av}(k)$ and its estimate $x_{av}(k|k)$, its input being a stack of the external signals and a constant for the controller's g^i term

$$\begin{bmatrix} x_{av}(k+1) \\ x_{av}(k+1\,|\,k+1) \end{bmatrix} = \begin{bmatrix} A^*_{av} & B^*_{av} f^{i}_{x} \\ M_{Kv} C^*_{av} A^*_{av} & A_{av} - M_{Kv} C_{av} A_{av} + B_{av} f^{i}_{x} + M_{Kv}\left(C^*_{av} B^*_{av} - C_{av} B_{av}\right) f^{i}_{x} \end{bmatrix} \begin{bmatrix} x_{av}(k) \\ x_{av}(k\,|\,k) \end{bmatrix}$$
$$+ \begin{bmatrix} G^*_{av} & 0 & B^*_{av} f^{i}_{r} & B^*_{av} g^{i} \\ M_{Kv} C^*_{av} G^*_{av} & M_{Kv} & B_{av} f^{i}_{r} + M_{Kv}\left(C^*_{av} B^*_{av} - C_{av} B_{av}\right) f^{i}_{r} & B_{av} g^{i} + M_{Kv}\left(C^*_{av} B^*_{av} - C_{av} B_{av}\right) g^{i} \end{bmatrix} \begin{bmatrix} w_{av}(k) \\ v(k+1) \\ y_r(k) \\ 1 \end{bmatrix} \quad (16)$$

$$y(k) = \begin{bmatrix} C^*_a & 0 \end{bmatrix} \begin{bmatrix} x_{av}(k) \\ x_{av}(k\,|\,k) \end{bmatrix} + \begin{bmatrix} 0 & q^{-1} & 0 & 0 \end{bmatrix} \begin{bmatrix} w_{av}(k) \\ v(k+1) \\ y_r(k) \\ 1 \end{bmatrix}, \qquad y_{\mathrm{nf}}(k) == \begin{bmatrix} C^*_a & 0 \end{bmatrix} \begin{bmatrix} x_{av}(k) \\ x_{av}(k\,|\,k) \end{bmatrix}$$

where q denotes the forward-shift operator. If the true model is equal to the nominal one, eq. (16) simplifies and the closed-loop poles of the system comprise the union of the controller poles $A_a + B_a f_x^i$ and the observer poles $A_a - M_K C_a A_a$ in the spirit of the Separation theorem ([31], p. 356).

The closed-loop system may be used with various forms of linear analysis: for step or impulse responses in the time domain, for root locus analysis on the complex plane, and for frequency domain analysis. The complementary sensitivity function $T(\omega)$ is the transfer function from the noise signal v to the noise-free measurement y_{nf}; it is obtained by extracting the appropriate part of eq. (16), transforming to the transfer function form, and shifting the numerator. The (output) sensitivity function $S(\omega)$ is the transfer function from v to the noisy measurement y; it is calculated using the relation $S(\omega) + T(\omega) = I$ (see Section 7.3 of [16], or [21] for more details). The same eq. (16) may be used for the analysis of the unconstrained region of the on-line MPC controller with $f_x^{uc} = -K_C N_N$, $f_r^{uc} = K_C I_{r_N}$, $g^{uc} = 0$, without mp-MPC partition calculation.

LLA is an extremely valuable supplementary tool for efficient tuning of the MPC controller and the estimator, used in addition to simulation analysis commonly performed with MPC. It allows better insight into the effects of the tuning parameters than simulation, and facilitates fast unconstrained analysis with very long horizons. When tuning, LLA is most useful for examining the performance in the unconstrained region, where the controller commonly dwells most of the time. In addition, with mp-MPC a similar analysis may be made for any other region where the controller tends to dwell. For engineering purposes, such analysis may be useful also for wider clusters of neighbouring regions with similar controller parameters. In addition, one may use the merged diagrams for all controller regions at once, for observing the influence of the tuning parameters on the whole cluster of controller regions and for detecting the outliers. For instance, one may plot a step response for any controller region, and the family of normalised step responses for all controller regions at once. These step responses are *strictly* only valid for step changes of small amplitudes, so that the process state does not leave the corresponding controller region. It may be argued that such analysis does not always make sense because the system does not settle in many of these regions; however, it still provides useful information about the local dynamic properties of the system. Further, using simulation analysis only one may overlook inappropriate behaviour under certain rarely encountered combinations of constraints, caused by an inappropriate choice of the MPC costs and horizons.

2.2 Modification for non-square plant

A modification of the typical tracking implementation with the joint scheme is required to address the issue of spare degrees of freedom when the plant has more inputs than outputs. A fixed reference u_{rf} may be imposed either on spare input(s) directly or on the corresponding additional state(s) $u(k-1)$ of the velocity-augmented model, and a relatively small cost weight R_u is added to this state in the cost function, so that the convergence towards u_{rf} is slow and the y_r tracking offset caused by this in the case of primary input saturation is hardly noticeable.

The cost function (8) is extended to

$$\begin{aligned} J\left(k, \Delta u_m(k)\right) &= e_N^T(.\,|\,k)\underline{\mathrm{Q}}_y e_N(.\,|\,k) + \Delta u_{N_u}^T(k)\underline{\mathrm{R}}_{\Delta u}\Delta u_{N_u}(k) \\ &\quad + e_{u,N}^T(.\,|\,k)\underline{\mathrm{R}}_u e_{u,N}(.\,|\,k) \end{aligned} \tag{17}$$

where $\underline{\mathrm{R}}_u = \mathrm{diag}(\underbrace{R_u, \ldots, R_u}_{N_u})$, and the additional error term for u is expressed in a similar form as (9), with an appropriate construction of N_U and S_U

$$e_{u,N}(.\,|\,k) = N_U x_{av}(k\,|\,k) + S_U \Delta u_{N_u}(k) - I_{m_N} u_r(k) \tag{18}$$

The controller gain definition (13) is extended to

$$\begin{aligned} K_C &= \begin{bmatrix} I_{n_u} & 0 & \ldots & 0 \end{bmatrix}\left(S_N^T \underline{\mathrm{Q}}_y S_N + S_U^T \underline{\mathrm{R}}_u S_U + \underline{\mathrm{R}}_{\Delta u}\right)^{-1} S_N^T \underline{\mathrm{Q}}_y \\ K_{C,U} &= \begin{bmatrix} I_{n_u} & 0 & \ldots & 0 \end{bmatrix}\left(S_N^T \underline{\mathrm{Q}}_y S_N + S_U^T \underline{\mathrm{R}}_u S_U + \underline{\mathrm{R}}_{\Delta u}\right)^{-1} S_U^T \underline{\mathrm{R}}_u \end{aligned} \tag{19}$$

and the receding-horizon control law in the unconstrained region becomes

$$\begin{aligned} \Delta u(k) &= \begin{bmatrix} K_C & K_{C,U} \end{bmatrix}\left(\begin{bmatrix} y_{r,N}(.\,|\,k) \\ u_{r,N}(.\,|\,k) \end{bmatrix} - \begin{bmatrix} N_N \\ N_U \end{bmatrix} x_{av}(k\,|\,k)\right) \\ &= \begin{bmatrix} K_C & K_{C,U} \end{bmatrix}\begin{bmatrix} -N_N & I_{r_N} \\ -N_U & 0 \end{bmatrix} x_{avt}(k\,|\,k) + K_{C,U} I_{r_N} u_r(k) \end{aligned} \tag{20}$$

3 Plasma annealer experimental case study

In our case study, mp-MPC is used to control the vacuum subsystem of a novel wire-annealing machine of PlasmaIt GmbH shown in Fig. 2. The machine heats the moving metal wire using magneto-focused plasma in an inert-gas atmosphere. The task of the controller is to maintain the specified pressure (y) in the plasma chamber of the annealer. The operating conditions may vary depending on the type of wire and the gas. The construction of the vacuum subsystem ensures that a certain pressure profile along the vacuum chamber is maintained to prevent any undesired leakage. The vacuum is maintained by several vacuum pumps, connected to different chambers in a cascade. Rough control of y is done by adjusting the input u_1, i.e., the frequency converters of the pumps connected to the chambers at the wire exit (right-hand side of Fig. 2). Fast regulation of disturbances is carried out by input u_2, a valve bypassing the sealing before the main chamber, with a five times faster response but a limited action range. The controller must be able to rapidly suppress any fast-acting disturbances that appear during operation, such as momentary sealing problems, the ignition of plasma, etc. It must also be able to operate over a wide range of operating points, affected by the diameter of the wire, the y_r set-point, the temperature during start-up, etc. Finally, it must be able to suppress the measurement noise efficiently.

*** FIG 2 HERE ***

The amplitude and rate constraints are present at both inputs: $0 < u_1 < 50$, $0 < u_2 < 10$, $-5\ \mathrm{s}^{-1} < \Delta u_1 < 5\ \mathrm{s}^{-1}$ and $-5\ \mathrm{s}^{-1} < \Delta u_2 < 5\ \mathrm{s}^{-1}$. The rate constraints become active at any significant actuator movement; however, with inadequate control, this may lead to an oscillatory response that is undetected by linear analysis. As there is one controlled output and two manipulated inputs, there is a spare degree of freedom, which is available when the constraints are inactive. It is reasonable to keep u_2 in the centre of its range when possible, so that the controller may effectively react to disturbances in any direction. Ignoring the spare degree of freedom may result in a poor coordination of the manipulated inputs and awkward control actions and poor conditioning of the control problem.

A previously existing control scheme with two PID controllers (2PID) comprises two loops: the fast loop attempts to control y to y_r by manipulating the valve position u_2; the slow loop drives u_2 towards the centre of its effective range $u_{2\mathrm{r}} = 3$. The tuning parameters $K_{\mathrm{P1}} = -0.5$, $T_{\mathrm{I1}} = 5$, $K_{\mathrm{P2}} = -1$, $T_{\mathrm{I2}} = 1$ were determined by manual experimental retuning after using the magnitude optimum tuning rules of [32]. Due to quantization noise (which is present because the operation is at the lower end of the measurement range), the derivative terms are not particularly useful.

It is evident that the process is of a nonlinear nature; however, as a challenge a simple mp-MPC replacement for the 2PID scheme, based on an identified low-order nominal model, is sought. The aim is to improve feedback performance while minding robustness to changes of operating conditions (modelling error). The following nominal discrete-time state-space model for model-based control design was obtained using identification from open-loop experimental signals about the operating point for $y_r = 5.0$ with the sampling time $T_S = 0.2$ s

$$A=\begin{bmatrix}0.8503 & 0 & 0 & 0\\ 0 & 0.9197 & 0 & 0\\ 0 & 0 & 0.6047 & 0\\ 0 & 0 & 0 & 0.7635\end{bmatrix},\ B=\begin{bmatrix}-0.6056 & 0\\ -0.5298 & 0\\ 0 & -0.3650\\ 0 & -0.2526\end{bmatrix} \qquad (21)$$
$$C=\begin{bmatrix}-0.1845 & 0.2191 & -2.1318 & 3.435\end{bmatrix},\ D=\begin{bmatrix}0 & 0\end{bmatrix}$$

with 2nd-order dynamics in each input branch, and the steady-state gain [–0.7 –1.7]. The set of models for robustness analysis using LLA or simulation includes models for the operating points $y_r = 2.9$ and $y_r = 7.0$, where the same dynamics are used, but the steady-state gain is changed to [–0.32 –1] and [–1.0 –2.4], respectively. Additionally, two similar models with one more sample of time delay are included in the set.

Intensive simulation testing of the mp-MPC controllers was performed prior to their experimental application, although simulation results are omitted due to the limited space. Aside from the nominal dynamics in eq. (21), the simulation model optionally includes rough estimates of the input static nonlinearities, signal quantisation, and measurement noise.

4 Controller tuning

In this first tuning step the following parameters for the joint scheme controller are selected: the sampling time T_S, the prediction horizon N, the control horizon N_u, the control move cost $R_{\Delta u}$, and the additional input cost R_u; the output cost Q_y is fixed at 1. While tuning, step responses to the reference and disturbance signals (assuming measured states) and the (dominant) controller pole positions are observed. Initially, this is done using LLA for the unconstrained region; subsequently, the mp-MPC controller is calculated and the constrained performance is verified. Various root locus diagrams obtained using LLA are extremely valuable, because they may help to explain unexpected effects of the tuning parameters.

The following values were selected for the parameters: $T_S = 0.2$ s, $N = 27$, $N_u = 2$, $R_{\Delta u} = [0.1\ 0;\ 0\ 0.05]$; the spare degree of freedom is handled with $u_{2\mathrm{rf}} = 3$ and $R_u = [0\ 0;\ 0\ 0.02]$. The disturbance-augmented state includes four original model states $x_1(k)$... $x_4(k)$ and one disturbance-estimation state $d(k)$. Along with the two previous inputs $u_1(k–1)$ and $u_2(k–1)$ due to the velocity form and the set-point $y_r(k)$, the total number of mp-MPC controller parameters is eight. A controller partition comprising 300 regions was computed in 30 s on a P-M@2GHz laptop computer using the MPT toolbox. Notice that the number of regions and the computation time are influenced by the bounds of the parameter space that are negotiable. The horizons were originally set using conventional rules of thumb. The choice of N_u is constrained by the designer's patience; at $N_u = 3$, 2800 regions are generated in 500 s. T_S is relatively short to allow rapid suppression of disturbances; therefore, a long N is required. Short N values tend to result in an undesirable constrained performance, while very long values cause a decrease in the $T(\omega)$ bandwidth; with the chosen N_u, N is fine-tuned using LLA of the unconstrained region to achieve desirable dominant pole locations near critical damping. A higher bandwidth may be achieved by longer (or infinite) N_u, but it may not be desired considering robustness to model inaccuracy.

With the mp-MPC controller partition determined, one may examine the nominal controller closed-loop dynamics $A_a+B_a f_x^i$ provided by LLA. The position of the poles of the controller is of interest because near-critical damping of the dominant poles and reasonable placement of all poles are desired. Figs. 3 and 4 show the nominal controller poles for all controller regions at once (the poles exactly at $1+j0$ belong to the velocity form integrators and should be ignored). For a detailed examination of specific regions, a separate diagram for each region may be plotted; however, the merged diagram of all regions is convenient for observing the overall *pattern* of changes when adjusting the tuning parameters and for finding the outliers. With the preferred choice $N = 27$ in Fig. 3, there is a single dominant pole in the unconstrained region, and the placement of the other poles is acceptable. With $N = 17$ in Fig. 4, there is a dominant pair of poles in the unconstrained region indicating an overshoot in the step response; some of the poles in the constrained regions are undesirably underdamped. The performance with the shorter horizon may be modified by increasing the control cost $R_{\Delta u}$, however the less desirable positioning of some of the poles in the constrained regions remains; similar conclusions may be reached using simulation analysis.

*** FIGS 3 AND 4 HERE ***

4.1 Simulation example

Fig. 5 displays a simplified mp-MPC simulation example to illustrate of the role of LLA in controller tuning. A single step change of the set-point from 3 to 9 is shown. The simulation is disturbance-free, with the nominal model (21) from the operating point for $y_r = 5.0$ used in place of the process. The mp-MPC controller with $N = 17$ (Fig. 4) is used.

*** FIG 5 HERE ***

Table 1 lists the controller regions visited during the step change in Fig. 5. Before the step change, the controller is in the unconstrained region 1; the corresponding controller poles are labelled with black × in Fig. 4. Shortly after the step change, the controller briefly passes through the constrained regions 229 and 123, and then stays for six samples in regions 122 and 58. All these regions are constrained regions with different combinations of rate and amplitude constraints at u_1 and/or u_2, where the controller output is saturated and LLA shows open-loop system dynamic. This is followed by a brief transition through the regions 8 and 18 where u_1 is no longer rate-limited but u_2 remains at the lower amplitude constraint. For these regions (including 14 other regions with free u_1 and saturated u_2), LLA indicates underdamped positions of the dominant poles near 0.85±0.25i. With the chosen MPC cost matrices this is not a problem in practice; R_u is chosen so that u_2 returns towards $u_{2\text{rf}}$ as soon as u_1 can take over, therefore such states are transient. However, with different tuning this may cause obvious performance degradation in such constraint conditions. At time 103.4 s, the controller enters region 2 where the immediate control move $u(k)$ is unconstrained, however $u_1(k+1|k)$ is at the lower amplitude constraint; LLA shows near-unconstrained dynamics. Finally, u_1 reaches the lower amplitude constraint at time 110.8 s and the controller enters region 17. In region 17, LLA shows near-unconstrained controller dynamics for the u_2 branch, and open-loop dynamics for the u_1 branch. A small tracking offset is detected (invisible in Fig. 5), due to the use of the R_u cost and the saturation of u_1.

Table 1. Regions of the mp-MPC controller visited during the step change simulation in Fig. 5.

Time	Region	Constraints*	f_x^i							f_r^i	g^i
											Controller poles (LLA)
95.0	1	none	0.0074	-0.0069	0.0293	-0.0669	0.1112	-0.0993	-0.0335	-0.1112	-1.3123
			-0.0327	0.0698	-0.0562	0.1902	1.1196	-0.0671	-0.9842	-1.1196	0.0042
			0.0166 0.5963±0.1225i 0.8478 0.9073±0.0767i								
100.0	229	3, 6, 12, 13	0	0	0	0	0	0	0	0	-1.0000
			0	0	0	0	0	0	0	0	-1.0000
			0.6047 0.7635 0.8503 0.9197 1 1								
100.2	123	3, 12, 13	0	0	0	0	0	0	0	0	-1.0000
			0	0	0	0	0	0	0	0	-1.0000
			0.6047 0.7635 0.8503 0.9197 1 1								
100.6	122	3, 9, 12	0	0	0	0	0	0	0	0	-1.0000
			0	0	0	0	0	0	-1.0000	0	0
			0 0.6047 0.7635 0.8503 0.9197 1								
101.8	58	9, 12	0	0	0	0	0	0	0	0	-1.0000
			0	0	0	0	0	0	-1.0000	0	0
			0 0.6047 0.7635 0.8503 0.9197 1								
103.0	8	9	-0.0622	0.1415	-0.0902	0.3373	2.4905	-0.2418	0	-2.4905	-1.3034
			0	0	0	0	0	0	-1.0000	0	0
			0 0.6047 0.7434 0.7635 0.8580±0.2480i								
103.2	18	2, 9	-0.0666	0.1515	-0.0929	0.3582	2.6142	-0.2836	0	-2.6142	-0.8543
			0	0	0	0	0	0	-1.0000	0	0
			0 0.6047 0.7314 0.7635 0.8407±0.2434i								
103.4	2	2	0.0094	-0.0110	0.0356	-0.0817	0.0243	-0.1141	-0.0358	-0.0243	-1.0511
			-0.0321	0.0686	-0.0543	0.1857	1.0934	-0.0715	-0.9849	-1.0934	0.0831
			0.0152 0.5998±0.1190i 0.8522 0.8969±0.0662i								
110.8	17	2, 8	0	0	0	0	0	-1.0000	0	0	0
			-0.0313	0.0677	-0.0514	0.1791	1.0953	0	-0.9878	-1.0953	-0.0018
			0 0.0152 0.5972±0.1202i 0.8503 0.9197								

* Constraints: rows of the constraints matrices defining CR^i in (15) (only those appearing in the table listed, out of 30):
2: $u_1(k+1|k)$ amplitude (min)
3: $u_2(k+1|k)$ amplitude (min)
6: $u_1(k+1|k)$ rate (down)
8: $u_1(k|k)$ amplitude (min)
9: $u_2(k|k)$ amplitude (min)
12: $u_1(k|k)$ rate (down)
13: $u_2(k|k)$ rate (down)

5 Estimator tuning

In this tuning step the disturbance-augmentation type and the observer pole positions or the KF covariance matrices Q_K and R_K are selected, where several specific parameterization forms may be used. The practical aim is to find a balanced compromise of the feedback responses to the process noise, the input disturbances, and the output disturbances; with acceptable results also with plant-to-model mismatch (over the whole operating range). While tuning, the closed-loop system dynamics with a set of candidate true models are studied using simulation, the root locus diagram and sensitivity functions diagrams. In sensitivity functions, the bandwidth of $T(\omega)$ and its roll-off at high frequencies (noise attenuation), the disturbance suppression in $S(\omega)$ at low and medium frequencies, and the resonance peaks near the bandwidth are observed.

From the theoretical point of view, a pole-placement observer appears to be a simple solution to the output-feedback problem. However, one should guess where the poles should actually be placed. One general recommendation suggests that the observer dynamics should be faster than the controller dynamics, so that the estimation error vanishes quickly enough for the controller to work properly. Unfortunately, the stability margins of the closed-loop system with LQG control may be reduced by such tuning [33]. This was also observed in our case study. An analysis of the closed-loop system properties with the set of candidate plant models was performed [21]. It does not appear possible to find any set of faster pole locations that would not result in a considerable deviation of the actual sensitivity function courses from the nominal ones. Similarly, the sets of closed-loop system poles with candidate "true" plant models would be dispersed far away from their nominal positions on the complex plane. Even with slower dynamics, a manual search was not particularly efficient. However, due to the small number of parameters this approach may be suitable for automated robustness optimization approaches, after the optimization constraints are properly defined.

The next starting point is the well-known output-step disturbance (OSD) model, obtained by selecting the disturbance augmentation at the output, Q_K = diag([0 ... 0 1]), and by fine-tuning the noise filter with $R_K = 0.01$. The resulting sensitivity functions are shown in Fig. 6. An inspection of the estimator poles reveals a slow pole on the real axis, which agrees with the findings of [28]. Compared to the sensitivity functions of the original 2PID scheme in Fig. 7, this OSD tuning shows a lower bandwidth and less aggressive suppression of disturbances, but the lower resonance peaks indicate better robustness to modelling error. The experimental control results of the OSD tuning are shown in Fig. 8 for the nominal set-point $y_r = 2.9$ and in Fig. 9 for the high-gain set-point $y_r = 7$. In Figures 10 and 11, the experimental performance of the original 2PID scheme in the same operating points is shown. The sequence of bidirectional step changes of amplitude 0.5, used in all the control experiments is: y_r reference at time 40 s, followed by u_1 disturbance at 80 s, u_2 disturbance at 120 s, and y disturbance at 160 s (a positive step change being always followed by a negative one). The 2PID scheme performs reasonably well, however it has an undesired tendency to overshoot, the variance of the control signals is higher than desired, and the responses in the high-gain set-point $y_r = 7$ are underdamped. With the mp-MPC controller with OSD tuning, the noise suppression is improved, so there is less variance in the control signals. There is also better damping during the transients at $y_r = 7$, where the process gain is increased. The bandwidth is lower, but the response is still reasonably fast. It is possible to retune the 2PID scheme for a similar noise suppression and robustness to gain variation by reducing K_{P2} to –0.5, but at the cost of a similarly decreased bandwidth. When tuned to a comparable bandwidth, the mp-MPC/OSD controller only has a slight advantage of lower overshoot. Conversely, the OSD feedback approach may not be retuned for much more aggressive response.

*** FIGS 6 AND 7 HERE SIDE-BY-SIDE ***

*** FIGS 8 AND 9 HERE SIDE-BY-SIDE, BELOW THEM FIGS 10 AND 11 SIDE-BY-SIDE ***

Improving the robustness to the modelling error was considered very important. This may be obtained by applying the concepts of "loop-transfer recovery" (LQG/LTR) [33]. For our case study the approach of recovery at the process input is convenient. By choosing $Q_K = B_a B_a^T$ and R_K to be very small, the closed-loop poles of the set of actual models indeed gather around the nominal controller poles. However, there is no integral action, as the noise covariance to the uncontrollable disturbance estimation state is zero with such tuning. By tuning a combination of OSD and LTR with $Q_K = B_a B_a^T + \mathrm{diag}([0 \ldots 0\ k_d])$, where the additional parameter k_d is used to tune the integral action, the robustness at the same level of performance can be only slightly improved, compared to the OSD model. Tuning Q_K and R_K using covariance estimation (and manual tuning of the integral action) was also attempted, with very similar results.

Finally, with some applications the feedback performance may be improved considerably by using the input-step disturbance (ISD) model; ISD may also be blended with LTR or covariance estimation based tuning. Fig. 12 shows the sigma diagram for $Q_K = B_a B_a^T + \mathrm{diag}([0 \ldots 0\ 1])$ and $R_K = 0.01$. Nominal LLA results generally show an improvement: the $T(\omega)$ bandwidth is increased, and there is better suppression of the disturbances in the low-frequency range in $S(\omega)$; there is more overshoot in the response to the output disturbances. However the robustness to plant-to-model mismatch is reduced, therefore ISD tuning was rejected.

*** FIG 12 HERE ***

6 Discussion

Stable control was also achieved with a simpler mp-MPC controller with first-order dynamics in each model branch, but considerable detuning was required and the results were not competitive with those of the 2PID scheme. A similar conclusion was reached when using the tracking error integration approach instead of disturbance estimation [15].

The presented output-feedback tracking concept can be extended to piecewise-affine (PWA) hybrid systems with no binary inputs, by using a modified hybrid form of the Kalman estimator that adjusts the estimator gain with respect to the currently active dynamic [34]. While this may appear to be an appealing possibility for the practical implementation of control for hybrid and also nonlinear processes, it should be noted that the resulting controllers may suffer from *short-sightedness,* like with attempts to use mp-MPC with constrained linear systems that have large dimensions. Within a reasonable time, such problems may only be solved off-line with very short horizons; this makes tuning difficult and efficient handling of state and output constraints practically impossible. With short horizons, infinite-horizon extensions of the cost function are valuable for the construction of a practically meaningful cost function, but do not help for long-term handling of constraints.

When long horizons are required for the sake of output or state constraints and fast sampling is preferred for the sake of efficient disturbance rejection, the tractability of the off-line computation may be regained by control move blocking and/or by placing the constraints sparsely over the prediction horizon [35]. While this may be considered sub-optimal, the optimality of a controller with slow sampling may as well be an illusion.

It was found that the mp-QP solvers of the MPT and HT toolboxes, used for the computation of the mp-MPC controller, are incapable of solving certain other more challenging mp-MPC control problems satisfactorily, which is due to a number of degeneracy-handling and numerical issues in the mp-QP solver [35]. However, the mp-QP solver issues are outside the scope of this paper.

7 Conclusions

It is shown that the disturbance-estimation based offset-free tracking schemes involving an observer/estimator, known from on-line MPC, are also applicable in mp-MPC. Further, that a "joint"-scheme, in which the MPC controller integrates the functions of constrained dynamic control and offset-free tracking without using a separate target calculator, may be efficiently used for control of small-scale multivariable processes with redundant control inputs. Such schemes facilitate tuning for efficient disturbance rejection and robustness, which is extremely important in low-level control applications. Local linear analysis was found to be an extremely valuable tool for tuning and performance analysis of the feedback action. However, the results of the case study also indicate that the improvements may not come as easily as some optimistic references predict [5]. With the tuning preference on the robust side of the performance/robustness trade-off, a relatively small improvement over the original two-loop PID control scheme in the form of lower overshoot was achieved at roughly the same response speed. There is also a certain improvement in the constrained performance compared to PID anti-windup, and a better insight into the constrained performance is available due to the explicit form of the mp-MPC control law. More significant practical advantages are expected in applications where output constraints or measured disturbances are important, or where PID-based control is less efficient due to more demanding process dynamics.

Acknowledgments

The authors are grateful for support of PlasmaIt GmbH (Lebring, AT) and Gregor Dolanc regarding plant modelling and experimentation. This work was supported in part by the EC (CONNECT, COOP-CT-2006-031638) and the Slovenian Research Agency (P2-0001, L2-2342).

References

[1] Qin, S. J., and Badgwell, T. A., "A survey of industrial model predictive control technology". *Control Engineering Practice*, 2003, 11, pp. 733–764.

[2] Richalet, J., "Industrial applications of model based predictive control". *Automatica*, 1993, 29, (5), pp. 1251–1274.

[3] Pistikopoulos, E. N., Dua, V., Bozinis, N. A., Bemporad, A., and Morari, M., "On-line optimization via off-line parametric optimization tools". *Computers and Chemical Engineering*, 2000, 24, pp. 183–188.

[4] Bemporad, A., Morari, M., Dua, V., and Pistikopoulos, E. N., "The explicit linear quadratic regulator for constrained systems". *Automatica*, 2002, 38, (1), pp. 3–20.

[5] Pannocchia, G., Laachi, N., and Rawlings, J. B.: "A candidate to replace pid control: Siso-constrained lq control". *AIChE Journal*, 2006, 51, pp. 1178–1189.

[6] Pistikopoulos, E. N., Georgiadis, M. C., and Dua, V., Eds.: "*Multi-Parametric Model-Based Control*". Wiley-VCH, Weinheim, 2007.

[7] Johansen, T. A., Jackson, W., Schreiber, R., and Tøndel, P.: "Hardware synthesis of explicit model predictive controllers". *IEEE Transactions on Control Systems Technology*, 2007, 15, pp. 191–197.

[8] Zeilinger, M. N., Jones, C.N., and Morari, M.: "Real-time suboptimal Model Predictive Control using a combination of Explicit MPC and Online Optimization". *IEEE Transactions on Automatic Control*, 2011, to appear.

[9] Kvasnica, M., Grieder, P., and Baotić, M.: "Multi-parametric toolbox". http://control.ee.ethz.ch/mpt/, accessed April 2011.

[10] Kvasnica, M.: "*Real-time model predictive control via multi-parametric programming*". VDM verlag, Saarbrücken, 2009.

[11] Bemporad, A.: "Hybrid toolbox for real-time applications, user's guide". Technical report, University of Siena, 2006.

[12] Pannocchia, G., and Rawlings, J. B.: "Disturbance models for offset-free model predictive control". *AIChE Journal*, 2003, 49, pp. 426–437.

[13] Grancharova, A., Johansen, T. A., and Kocijan, J.: "Explicit model predictive control of gas-liquid separation plant via orthogonal search tree partitioning". *Computers and Chemical Engineering*, 2004, 28, pp. 2481–2491.

[14] Sakizlis, V., Kakalis, N. M. P., Dua, V., Perkins, J. D., and Pistikopoulos, E. N.: "Design of robust model-based controllers via parametric programming". *Automatica*, 2004, 40, pp. 189–201.

[15] Pregelj, B., and Gerkšič, S.: "Tracking implementations in multi-parametric predictive control". Proc. 8th Portuguese Conference on Automatic Control CONTROLO 2008, Universidade de Trás-os-Montes e Alto Douro, Vila Real, 2008, pp. 944–949. Online: http://dsc.ijs.si/files/papers/PG_CONTROLO08.pdf

[16] Maciejowski, J. M.: "*Predictive Control with Constraints*". Prentice Hall, Harlow UK, 2002.

[17] Muske, K. R., and Badgwell, T. A.: "Disturbance modeling for offset-free linear model predictive control". *Journal of Process Control*, 2002, 12, pp. 617–632.

[18] Odelson, B. J., Rajamani, M. R., and Rawlings, J. B.: "A new autocovariance least-squares method for estimating noise covariances". *Automatica*, 2006, 42, pp. 303–308.

[19] Darby, M. L., and Nikolaou, M.: "A parametric programming approach to moving horizon state estimation". *Automatica*, 43, pp. 885–891, 2007.

[20] Sui, D., Feng, L., and Hovd, M.: "Robust output feedback model predictive control for linear systems via moving horizon estimation". *Proc. 2008 American Control Conference*, Seattle WA, 2008, pp. 453–458.

[21] Gerkšič, S., Strmčnik, S., and van den Boom, T. J. J.: "Feedback action in predictive control: an experimental case study". *Control Engineering Practice*, 2008, 16, pp. 321–332.

[22] González, A. H., Adam, E. J., and Marchetti, J. L.: "Conditions for offset elimination in receding horizon controllers: A tutorial analysis". *Chemical Engineering and Processing*, 2008, 47, pp. 2184–2194.

[23] Sakizlis, V., Dua, V., Perkins, J. D., and Pistikopoulos, E. N.: "Robust model-based tracking control using parametric programming". *Computers and Chemical Engineering*, 2004, 28, pp. 195–207.

[24] Sakizlis, V.: "*Design of model based controllers via parametric programming*". PhD thesis, Imperial College, London, 2003.

[25] Muske, K. R. and Rawlings, J. B.: "Model predictive control with linear models". *AIChE Journal*, 1993, 39, pp. 262–287.

[26] Rao, C. V., and Rawlings, J. B.: "Steady States and Constraints in Model Predictive Control". *AIChE Journal*, 1999, 45, pp. 1266–1278.

[27] Limon, D., Alvarado, I., Alamo, T., and Camacho, E. F.: "MPC for tracking piecewise constant references for constrained linear systems". *Automatica*, 2008, 44, pp. 2382–2387.

[28] Bageshwar, V. L., and Borrelli, F.: "On a property of a class of offset-free model predictive controllers". *IEEE Transactions on Automatic Control*, 2009, 54, pp. 663–669.

[29] Jones, C. N. and Morari, M.: "Multiparametric linear complementarity problems". Proc. 45th IEEE Conference on Decision and Control, 2006, pp. 5687–5692.

[30] Lee, J. H., Yu, Z. H.: Tuning of model predictive controllers for robust performance. *Computers & Chemical Engineering*, 1994, 18, pp. 15–37.

[31] Åström, K. J. and Wittenmark, B.: "*Computer Controlled Systems: Theory and Design*", 2nd edn. Prentice-Hall, Englewood Cliffs, NJ, 1990.

[32] Vrančić, D., Peng, Y., and Strmčnik, S.: "A new PID controller tuning method based on multiple integrations", *Control Engineering Practice*, 1999, 7, (5), pp. 623–633.

[33] Maciejowski, J. M., *Multivariable Feedback Design*. Addison-Wesley, Wokingham UK, 1989.

[34] Pregelj, B., and Gerkšič, S.: "Hybrid explicit model predictive control of a nonlinear process approximated with a piecewise affine model". *Journal of Process Control*, 2010, 20, pp. 832–839.

[35] Gerkšič, S.: "Improving Reliability of Partition Computation in Explicit MPC with MPT Toolbox". Proc. IFAC 18th World Congress, Milano, 2011, pp. 9260-9265.

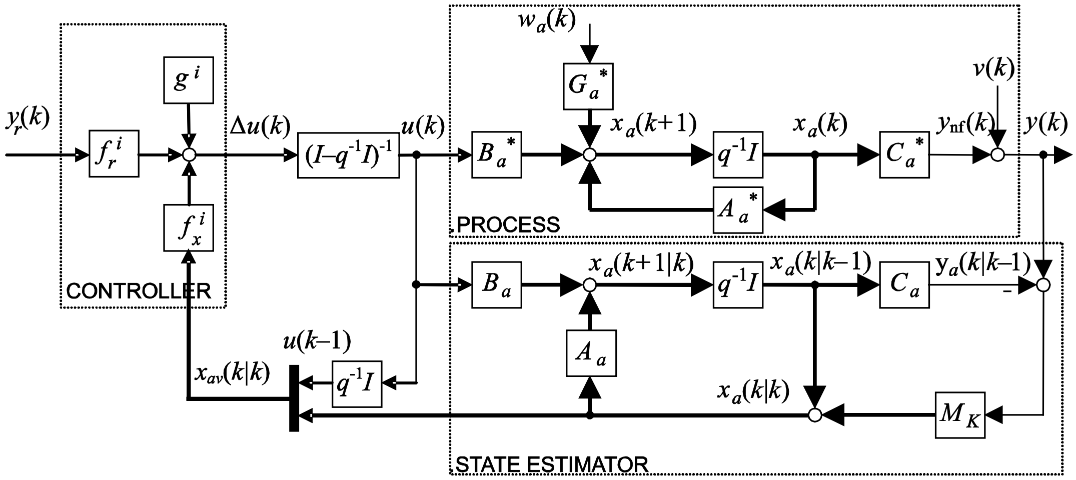

Fig. 1. Schematic diagram of closed-loop system with mp-MPC.

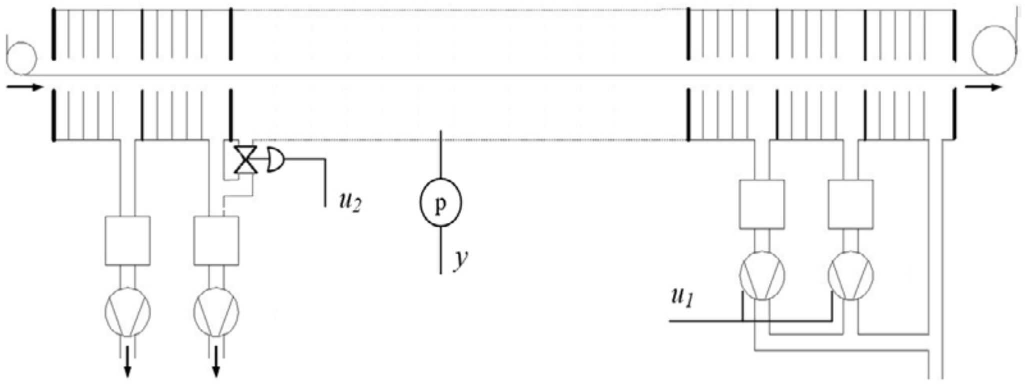

Fig. 2. Vacuum subsystem of plasma annealer.

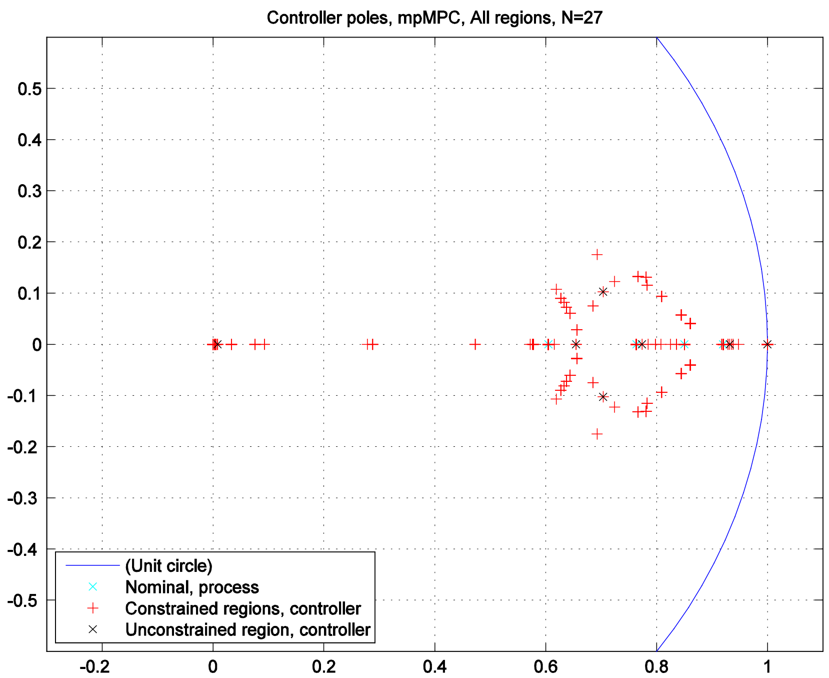

Fig. 3. Nominal controller closed-loop poles for all controller regions, N = 27

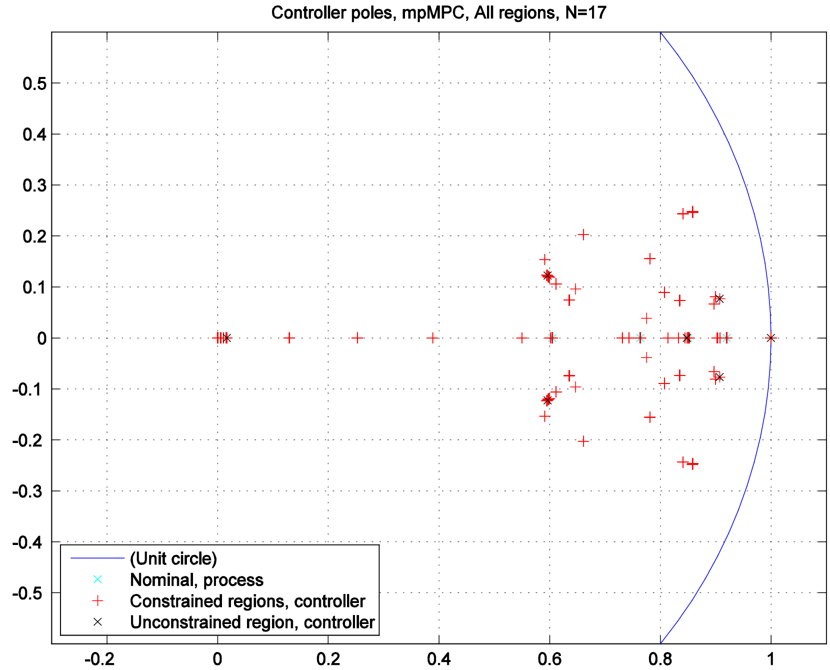

Fig. 4. Nominal controller closed-loop poles for all controller regions, $N = 17$

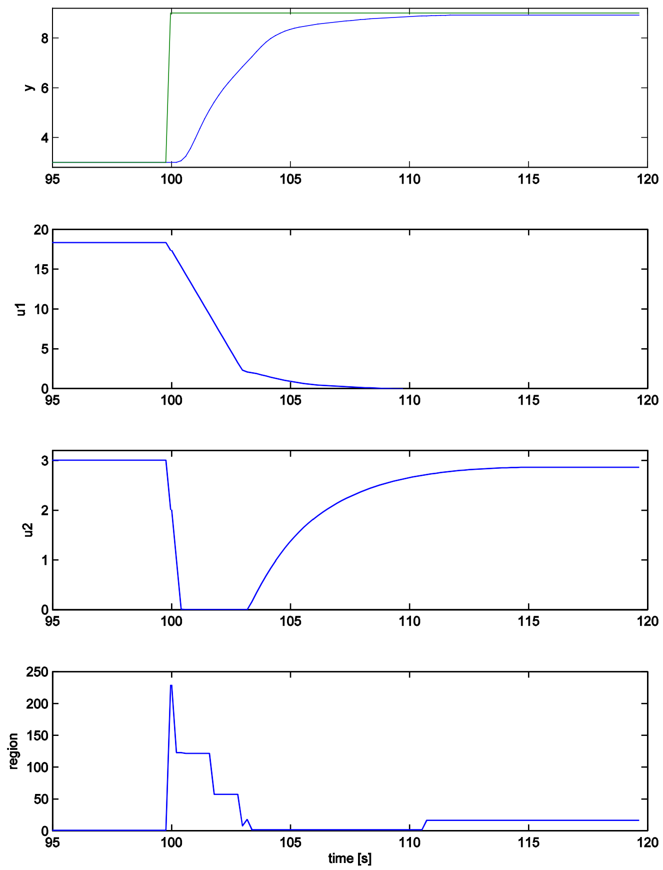

Fig. 5. Simulated mp-MPC response to a large step change of the set-point signal.

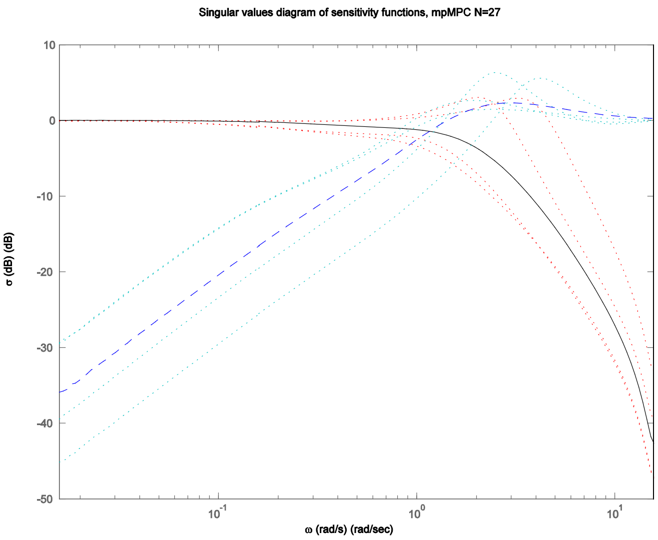

Fig. 6. Sigma diagram of nominal $S(\omega)$ (dashed) and $T(\omega)$ (solid), mp-MPC with OSD disturbance model. Dotted: set of true models.

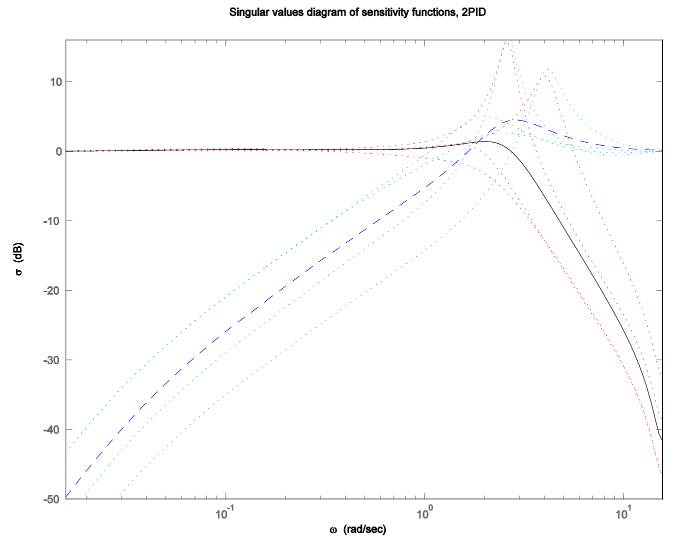

Fig. 7. Sigma diagram of nominal $S(\omega)$ (dashed) and $T(\omega)$ (solid), 2PID scheme. Dotted: set of true models.

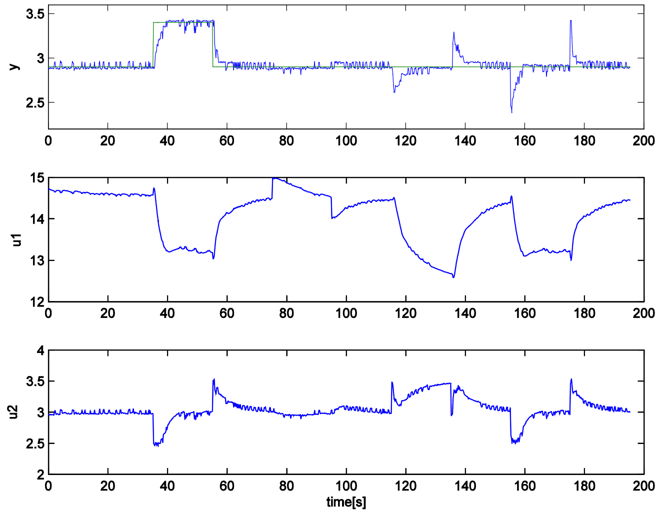

Fig. 8. mp-MPC + OSD, experiment, $y_r = 2.9$.

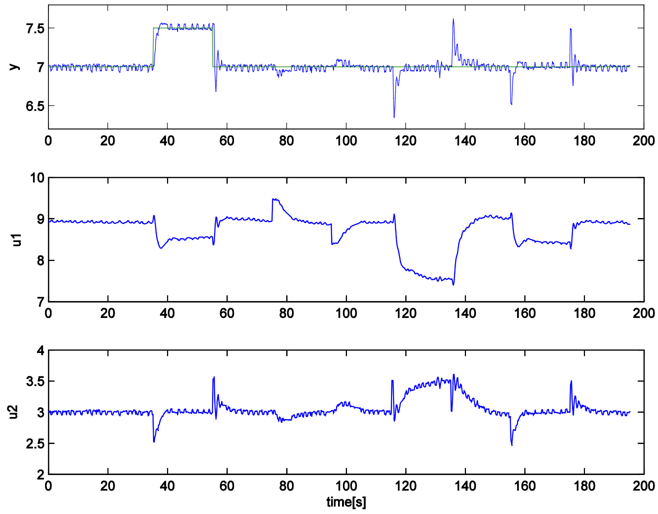

Fig. 9. mp-MPC + OSD, experiment, $y_r = 7$.

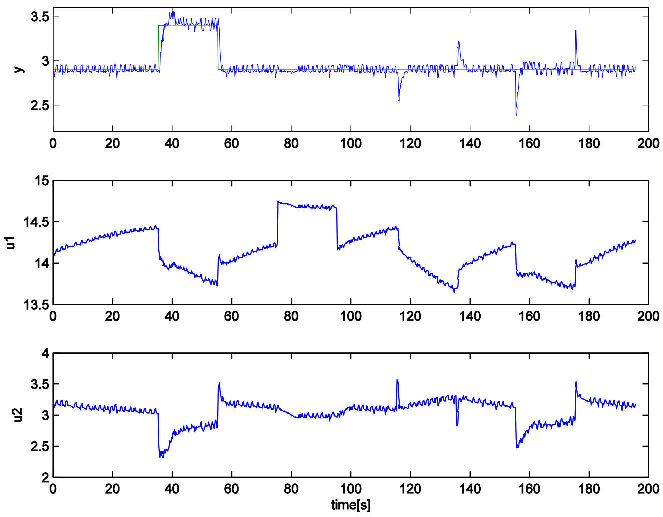

Fig. 10. 2PID scheme, experiment, $y_r = 2.9$.

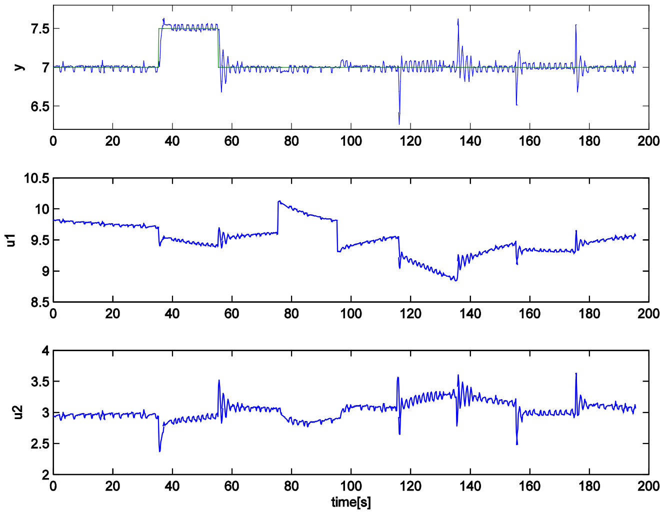

Fig. 11. 2PID scheme, experiment, $y_r = 7$.

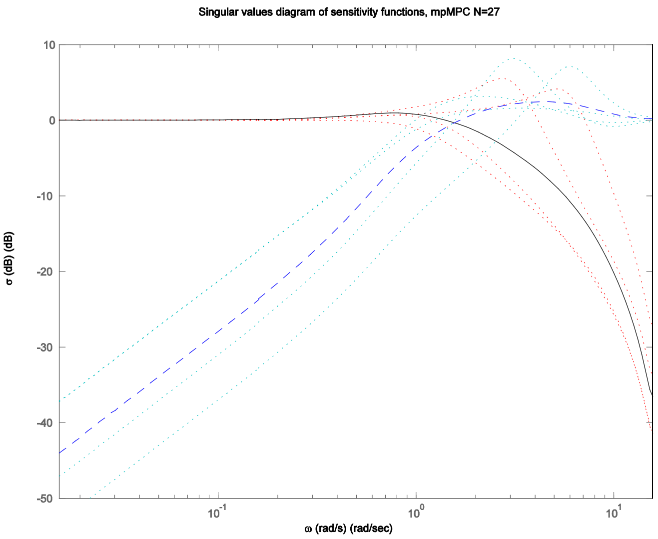

Fig. 12. Sigma diagram of nominal $S(\omega)$ (dashed) and $T(\omega)$ (solid), mp-MPC with ISD+LTR disturbance model. Dotted: set of true models.